

CrossMark
click for updatesCite this: *J. Mater. Chem. A*, 2016, 4, 16330Received 22nd June 2016
Accepted 25th September 2016

DOI: 10.1039/c6ta05254a

www.rsc.org/MaterialsA

A novel one-step synthesized and dopant-free hole transport material for efficient and stable perovskite solar cells†

Xiaoming Zhao,^{‡ae} Fei Zhang,^{‡abe} Chenyi Yi,^b Dongqin Bi,^b Xiangdong Bi,^c Peng Wei,^d Jingshan Luo,^b Xicheng Liu,^g Shirong Wang,^{*ae} Xianggao Li,^{ae} Shaik Mohammed Zakeeruddin^{*bf} and Michael Grätzel^{*b}

A hole transport material ST1 was synthesized by a one-step Heck reaction. Compared to Spiro-OMeTAD, perovskite solar cells with ST1 exhibit a remarkable overall power conversion efficiency of 15.4% without the use of any dopants and additives, which is comparable to that of the devices based on doped Spiro-OMeTAD (16.3%) and present better stability during a four week aging test.

Perovskite solar cells (PSCs) with methyl ammonium lead halides as light absorbers¹ have attracted considerable attention because of their simple structures, low fabrication cost and high power conversion efficiencies (PCEs).^{2–5} Recently, PSCs have shown a rapid increase of PCE to over 21.0% by extensive optimization of metal oxide scaffolds and device processing conditions using 2,2',7,7'-tetrakis(*N,N'*-di-*p*-methoxyphenylamino)-9,9'-spirobiuorene (Spiro-OMeTAD) as the hole transport material.⁶ However, the Spiro-OMeTAD suffers from a complex synthetic approach and cumbersome purification, which might hamper its wide application in PSCs.⁷ In addition, it performs efficiently in PSCs only when it is doped with a metal complex and additives, which affects the long-term device stability.⁸

In this regard, it is highly desirable to develop new low-cost HTMs that are easy to prepare and to improve both the efficiency and stability of PSCs. Various kinds of inorganic semiconductors,⁹ organic small molecule semiconductors^{10–16} and conducting polymers^{17,18} have been reported as novel HTMs for PSCs with comparable efficiencies to those of Spiro-OMeTAD based devices. However, the drawback of these classical novel HTMs is the need for dopants to achieve good performance in PSCs, which may render the device unstable. To solve this problem, some dopant free HTMs have been developed for PSCs and have achieved a PCE of 18.6% using an HTM based on a C_{3h} symmetrical truxene core.^{15,19–24} However, only four small molecule dopant-free HTMs are reported with a PCE over 15% to date and these dopant-free HTMs suffer from multiple synthesis steps and expensive precursors, making them difficult to be produced on a larger scale.^{13,17,18,23} Therefore, efforts to develop dopant-free and facilely synthesized HTMs to replace Spiro-OMeTAD are still needed.

In this study, we present the synthesis and characterization of a novel dopant-free and facilely synthesized HTM, coded as ST1, as well as its application in PSCs. ST1 can be synthesized with a high yield of 86% by a one-step Heck reaction. PSCs fabricated with ST1 as the HTM achieve a PCE of 15.4% in the absence of dopants under AM 1.5G (100 mW cm⁻²) illumination, which matches that of p-doped Spiro-OMeTAD (16.3%). In addition, compared to devices based on Spiro-OMeTAD, ST1-based devices exhibit a better stability during a 4 week aging test. Therefore, ST1 has the potential to replace Spiro-OMeTAD as a viable HTM for low-cost and highly stable perovskite solar cells.

As shown in Fig. 1a, 4-(4-(bis(4-(4-(dibutylamino)styryl)phenyl)-amino)styryl)-*N,N*-dibutylaniline (ST1) was synthesized by a one-step Heck reaction of the inexpensive commercial precursors tris(4-bromophenyl)amine and *N,N*-dibutylaminostyrene. Compared to the synthesis of Spiro-OMeTAD which requires five steps,²⁵ ST1 can be synthesized by only one synthetic step, making the synthesis of ST1 easily scalable. An estimate of the cost of ST1 is made (Table S1, ESI†) by using the

^aSchool of Chemical Engineering and Technology, Tianjin University, 300072 Tianjin, China. E-mail: wangshirong@tju.edu.cn

^bLaboratory of Photonics and Interfaces, Institute of Chemical Sciences and Engineering, École Polytechnique Fédérale de Lausanne (EPFL), Station 6 CH-1015, Lausanne, Switzerland. E-mail: michael.gratzel@epfl.ch; shaik.zakeer@epfl.ch

^cDepartment of Physical Sciences, Charleston Southern University, 9200 University Blvd., Charleston, SC 29485, USA

^dAffinity Research Chemicals, Inc., 9 Germay Drive, Suite 300B, Wilmington, DE 19804, USA

^eCollaborative Innovation Center of Chemical Science and Engineering (Tianjin), 300072 Tianjin, China

^fCenter of Excellence for Advanced Materials Research (CEAMR), King Abdulaziz University, Jeddah, Saudi Arabia

^gQufu Normal University, School of Chemistry and Chemical Engineering, 273165 Qufu, China

† Electronic supplementary information (ESI) available: CV curves, TOF transients of ST1, stabilised power outputs, reproducibility tests of PSCs, and comparison table of recently reported dopant-free HTMs for PSC. See DOI: 10.1039/c6ta05254a

‡ X. M. Z. and F. Z. have equivalent contribution.

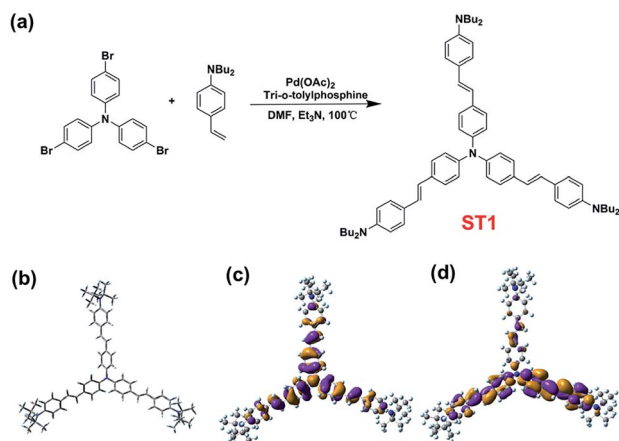


Fig. 1 (a) One-step synthetic route for ST1; (b) optimized molecular conformation; (c) HOMO and (d) LUMO orbitals obtained from DFT calculations.

cost model described in recently published literature studies for different hole transport materials.^{25,26} The total cost to obtain 1 gram of ST1 is much cheaper than the commercial price of Spiro-OMeTAD.²⁷ Synthesis details and full chemical characterization using ¹H NMR, ¹³C NMR, and mass spectrometry (MS) are provided in the Experimental section and Fig. S1–S3 (ESI).† The thermal properties of ST1 were tested *via* thermogravimetric analysis (TGA) and differential scanning calorimetry

(DSC) as shown in Fig. 2a. The TGA curve indicates that ST1 is thermally stable up to 400 °C and the DSC curve shows that the glass transition temperature (T_g) of ST1 is 100.3 °C which is lower than that of Spiro-OMeTAD ($T_d = 425$ °C, $T_g = 125$ °C) due to its smaller molecular size than Spiro-OMeTAD.^{28,29}

Density functional theory (DFT) calculations were employed to study the geometric and electronic properties of the novel HTM by using the Gaussian 09 program package at the B3LYP/6-31G(d)* level. The optimized molecular structures and frontier molecular orbitals of ST1 are shown in Fig. 1. The electron density distribution of the highest occupied molecular orbital (HOMO) of the ST1 is mainly located at the donor triphenylamine part with the linking phenylethylene units. The electron density distribution of the lowest unoccupied molecular orbital (LUMO) is primarily located at the phenylethylene units and the neighbouring benzene rings. This substantial overlapping between HOMO and LUMO orbitals can suppress charge recombination at the TiO₂/HTM interface.³⁰

Fig. 2b compares the UV-visible absorption and photoluminescence (PL) spectra of ST1 and Spiro-MeOTAD. In tetrahydrofuran (THF) solution, ST1 shows two absorption bands at around 332 nm and 404 nm while Spiro-MeOTAD shows two absorption bands at 304 nm and 377 nm. Compared with the absorption of Spiro-MeOTAD, ST1 shows a significant red-shifted onset of absorption and the absorption maximum. This can be ascribed to the more planar ground state geometry of the electron donating phenylenevinylene units caused by the lower degree of torsion due to C=C interactions. The PL spectra

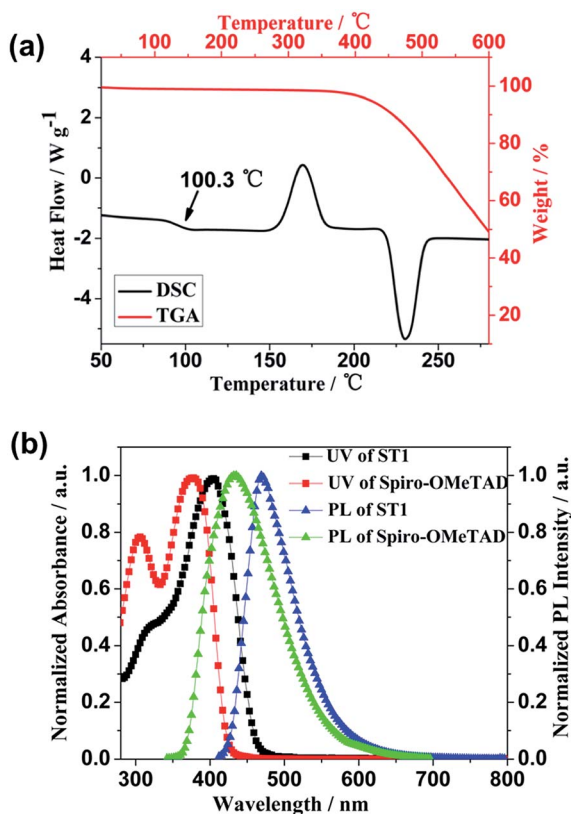


Fig. 2 (a) TGA and DSC curves of ST1; (b) UV-Vis absorption and photoluminescence spectra of ST1 and Spiro-OMeTAD in THF solution ($c = 1.0 \times 10^{-5}$ mol L⁻¹).

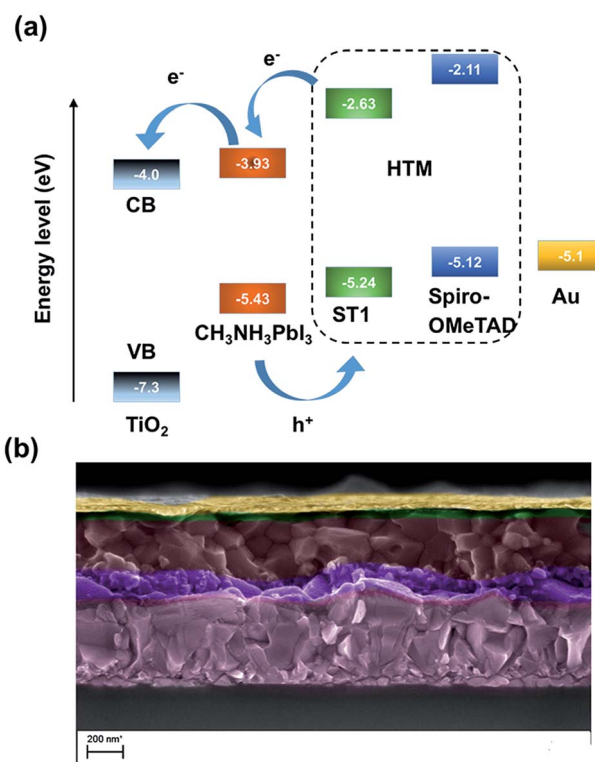


Fig. 3 (a) Energy level diagram of the components used in solar cells described; (b) cross-sectional SEM image of the investigated perovskite solar cells.

show maximum emission at 433 nm for Spiro-OMeTAD and 468 nm for ST1. Electrochemical measurements were performed in order to determine the HOMO and LUMO energy levels. The cyclic voltammograms (CVs) of ST1 and Spiro-OMeTAD are shown in Fig. S1.† From the CVs and UV-visible spectra, the HOMO energy levels of ST1 and Spiro-OMeTAD are -5.24 eV and -5.12 eV and the LUMO energy levels are -2.63 eV and -2.11 eV, respectively. Fig. 3a shows the relative energy levels of $\text{CH}_3\text{NH}_3\text{PbI}_3$ and HTMs. The HOMO of ST1 lies above that of $\text{CH}_3\text{NH}_3\text{PbI}_3$ (-5.43 eV), which provides sufficient driving force for hole injection from $\text{CH}_3\text{NH}_3\text{PbI}_3$ into the HTMs.³¹ The HOMO energy level of ST1 is ~ 120 mV lower than that of Spiro-OMeTAD, indicating that ST1 based devices can potentially generate a higher V_{oc} than Spiro-OMeTAD based devices.³² In addition, compared to $\text{CH}_3\text{NH}_3\text{PbI}_3$, the higher LUMO levels of ST1 (-2.63 eV) can block the electron transport from $\text{CH}_3\text{NH}_3\text{PbI}_3$ to the Au counter electrode to suppress the carrier recombination.³³

We determined the hole mobility of ST1 by using the time-of-flight (TOF) method following previous reports.³⁴ The TOF transient of ST1 is shown in Fig. S5.† The hole mobility of ST1 is $4.57 \times 10^{-4} \text{ cm}^2 \text{ V}^{-1} \text{ s}^{-1}$ at an electric field of $2.5 \times 10^5 \text{ V cm}^{-1}$, which is 2 times higher than that of Spiro-OMeTAD (2×10^{-4}

$\text{cm}^2 \text{ V}^{-1} \text{ s}^{-1}$ at an electric field of $2.6 \times 10^5 \text{ V cm}^{-1}$),¹⁰ which bodes well for its use in PSCs.

Fig. 3b shows the cross-sectional scanning electron microscopy (SEM) image of the investigated perovskite solar cells in which the $\text{CH}_3\text{NH}_3\text{PbI}_3$ perovskite layer was deposited on mesoporous- TiO_2 (mp- TiO_2) by the anti-solvent method described in the Experimental section (ESI).† After annealing of the perovskite film, HTMs were deposited by spin-coating followed by a deposition of a thin gold layer as the hole collector. As can be seen from the image, the $\text{CH}_3\text{NH}_3\text{PbI}_3$ perovskite penetrates into the mp- TiO_2 and forms an overlayer. Similarly, the HTMs blend into the pores in the TiO_2 /perovskite layer and form a thin capping layer on the top.

The photovoltaic performances of PSCs employing dopant-free ST1 as the HTM were measured under AM 1.5G (100 mW cm^{-2}) simulated light illumination. For comparison, a reference cell with Spiro-OMeTAD with a Li-TFSI dopant and 4-*tert*-butylpyridine (*t*-BP) additive was also fabricated under similar conditions. The series (R_s) resistance was calculated from the current-voltage (J - V) curves. Fig. 4a shows the current-voltage (J - V) characteristics obtained from PSCs using each HTM in different scan directions. The corresponding photovoltaic parameters are summarized in Table 1. The PCE of the PSC with

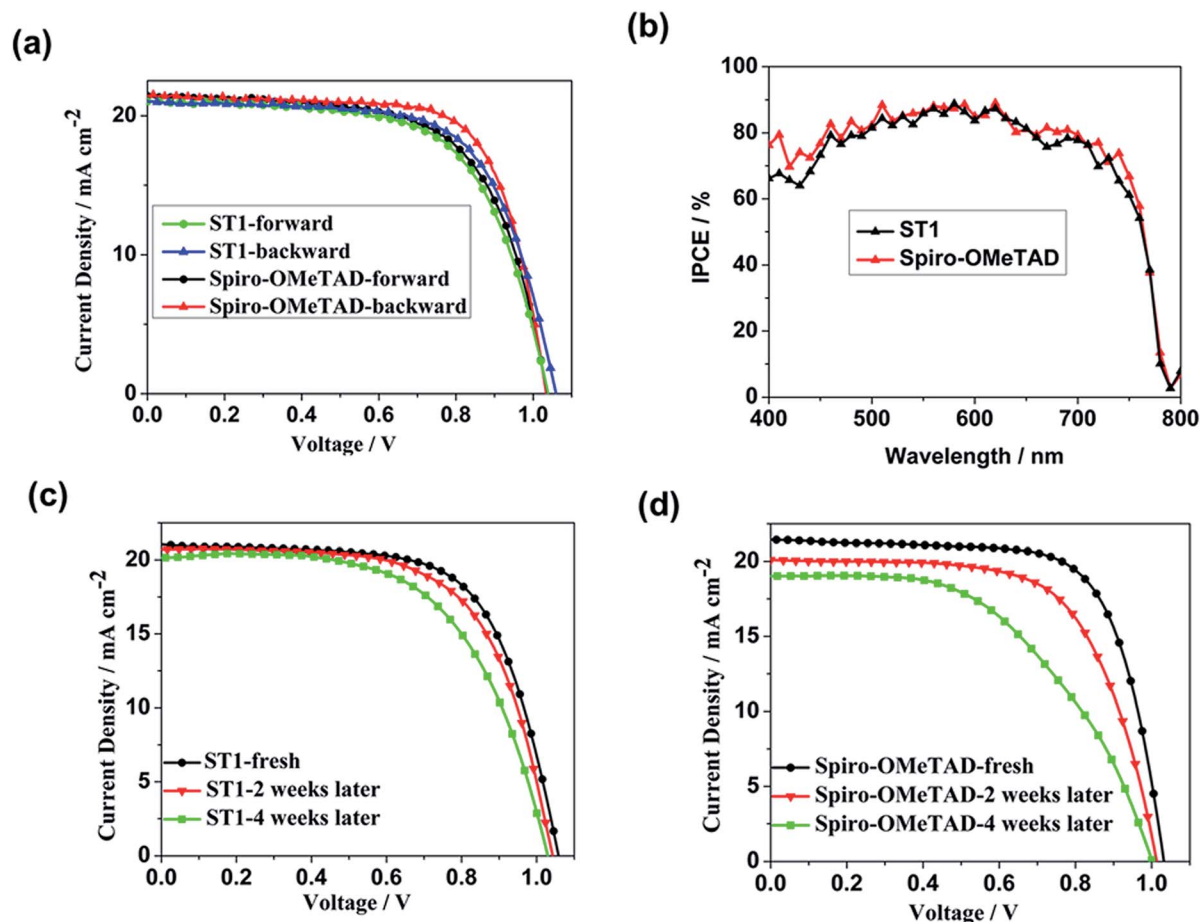


Fig. 4 (a) J - V curves and (b) IPCE spectra of PSCs fabricated with ST1 and Spiro-OMeTAD; J - V curves of PSCs fabricated with ST1 (c) and Spiro-OMeTAD (d) fresh, after 2 weeks and 4 weeks.

Table 1 Summary of photovoltaic parameters of the solar cells with ST1 and Spiro-OMeTAD as the HTMs evaluated under one sun conditions in different scan directions with a bias step of 5 mV

HTM	J_{sc} (mA cm^{-2})	V_{oc} (V)	FF	PCE (%)	R_s ($\Omega \text{ cm}^{-2}$)
Spiro-OMeTAD (backward)	21.41	1.034	0.71	16.3	12.15
Spiro-OMeTAD (forward)	21.43	1.035	0.65	14.9	24.04
ST1 (backward)	21.07	1.059	0.66	15.4	16.12
ST1 (forward)	21.02	1.039	0.64	14.5	36.56

dopant-free ST1 was 15.4%, with a short-circuit current density (J_{sc}) of 21.07 mA cm^{-2} , an open circuit voltage (V_{oc}) of 1.059 V, and a fill factor (FF) of 0.66. Under the same fabrication conditions, the cell based on Spiro-OMeTAD achieved a PCE of 16.3% with a J_{sc} of 21.41 mA cm^{-2} , a V_{oc} of 1.034 V, and an FF of 0.71. This higher V_{oc} of ST1-based devices may be attributed to the lower HOMO energy level of ST1. The relatively lower FF of ST1 can be well explained by its higher series resistances ($16.12 \Omega \text{ cm}^{-2}$) than Spiro-OMeTAD ($12.15 \Omega \text{ cm}^{-2}$).³⁵ The J - V curves of the PSC based on ST1 show a smaller hysteresis than that of Spiro-OMeTAD based devices. The measured PCE differences between the forward scan and the backward scan are 0.9% and 1.4% for the ST1 and Spiro-OMeTAD based devices, respectively. According to a recent report,^{36,37} slow kinetic processes such as charge transport or interfacial separation will lead to pronounced hysteresis. The devices based on ST1 are less pronounced in terms of hysteresis, which could be ascribed to their higher hole mobility that facilitates hole transport. As shown in Fig. S6,[†] the stabilized power outputs are 15.3% for ST1-based devices and 16.3% for Spiro-OMeTAD-based devices, which are consistent with the obtained PCEs. The lower J_{sc} values obtained for devices based on ST1 compared to those of Spiro-OMeTAD-based devices are in agreement with the incident photon-to-current conversion efficiency (IPCE) spectra shown in Fig. 4b. For statistical analysis, we fabricated a batch of 10 cells each with ST1 and Spiro-OMeTAD and examined the reproducibility of the cell performance. The data are tabulated in Fig. S7 and S8, of the ESI,[†] indicating good device reproducibility.

Stability is a critical factor for considering new HTM materials. To study the stability, PSCs based on the two HTMs were fabricated and tested under the same conditions for comparison. The unsealed devices were stored at room temperature in ambient air in the dark at 30% relative humidity. We measured the J - V curves after 2 and 4 weeks to monitor the stability. The results are shown in Fig. 4 and Table S2.[†] The PCEs of devices based on ST1 shows a decrease from 15.4% to 13.2% while the PCE of Spiro-OMeTAD-based devices decreased from 16.3% to 10.3%. The ST1 based devices exhibited a more stable performance than Spiro-OMeTAD-based devices over the 4 week aging time, which we attribute to the absence of additives. Additives such as Li-TFSI and *tert*-butyl pyridine (*t*-BP) are expected to have detrimental effects on cell stability since Li-TFSI promotes the oxidation of Spiro-OMeTAD by oxygen in the presence of light or heat and *t*-BP dissolves the perovskite.^{38,39}

To further demonstrate the improvement of ST1 for PSCs, we make a comparison of some recently reported small molecule dopant-free HTMs applied in PSCs. The synthetic steps and the corresponding parameters of the PSCs based on these HTMs are tabulated in Table S3.[†] Four HTMs Trux-OMeTAD, Z1011, Z1013 and DERDTS-TBDT present relatively high PCEs over 15% but their syntheses require 4, 8, 8 and 6 steps, respectively, which makes them difficult to be produced on a larger scale. SAF-OMe and DFTAB can be produced by fewer synthetic steps but the PCEs of the devices based on them are relatively low, which is 12.4% and 7.2%, respectively. The reported HTM in this paper, ST1, has the smallest molecular size among them and shows a comparable PCE to the high performance HTMs and can be synthesized by a facile one-step reaction, making it a promising candidate for low-cost and highly efficient perovskite solar cells.

Conclusions

In conclusion, a novel hole transport material ST1 was designed and prepared by a simple one-step synthesis method from commercial inexpensive precursors with a high yield. A PCE as high as 15.4% was achieved by applying undoped ST1 as the HTM in PSCs. Long-term stability studies in the dark showed that ST1-based devices are more stable when exposed to air than cells employing Spiro-OMeTAD. The low-cost, facile one-step synthetic method as well as the excellent hole mobility and appropriate energy level makes ST1 a promising candidate to substitute Spiro-OMeTAD in the large scale production of high-performance and stable perovskite solar cells.

Author contributions

XMZ measured all the physical property tests and quantum chemical calculations. FZ designed and performed the experimental study on device fabrication and basic characterization. XDB and PW designed and synthesized the novel HTMs. XCL performed the hole mobility measurements. CYY and DQB carried out the stability test. JSL performed SEM. XMZ wrote the draft of the paper. All the authors approved the paper. SMZ and XGL coordinated the research and SRW and MG supervised the project.

Acknowledgements

This work was supported by the National Natural Science Foundation of China (21676188) and the Key Projects in the Natural Science Foundation of Tianjin, China (16JCZDJC37100). FZ thanks the China Scholarship Council for funding. MG thanks the King Abdulaziz City for Science and Technology (KACST) for financial support. Financial support from the Swiss National Science Foundation (SNSF), the NRP 70 "Energy Turnaround", CCEM-CH in the 9th call proposal 906: CONNECT PV as well as from SNF-NanoTera and the Swiss Federal Office of Energy (SYNERGY) is gratefully acknowledged.

Notes and references

- 1 A. Kojima, K. Teshima, Y. Shirai and T. Miyasaka, *J. Am. Chem. Soc.*, 2009, **17**, 6050–6051.
- 2 F. Zhang, S. R. Wang, X. G. Li and Y. Xiao, *Synth. Met.*, 2016, **220**, 187–193.
- 3 J. Burschka, A. Dualah, F. Kessler, E. Baranoff, N. L. Cevey-Ha, C. Y. Yi, M. K. Nazeeruddin and M. Grätzel, *J. Am. Chem. Soc.*, 2011, **45**, 18042–18045.
- 4 J. Burschka, N. Pellet, S. J. Moon, R. Humphry-Baker, P. Gao, M. K. Nazeeruddin and M. Grätzel, *Nature*, 2013, **7458**, 316–319.
- 5 V. W. Bergmann, S. A. Weber, F. J. Ramos, M. K. Nazeeruddin, M. Grätzel, D. Li, A. L. Domanski, I. Lieberwirth, S. Ahmad and R. Berger, *Nat. Commun.*, 2014, **5**, 1–9.
- 6 F. Zhang, S. Wang, X. Li and Y. Xiao, *Curr. Nanosci.*, 2016, **2**, 137–156.
- 7 Y. Shi, K. Hou, Y. Wang, H. Ren, M. Peng, F. Chen and S. Zhang, *J. Mater. Chem. A*, 2016, **4**, 5415–5422.
- 8 J. Liu, Y. Wu, C. Qin, X. Yang, T. Yasuda, A. Islam, K. Zhang, W. Peng, W. Chen and L. Han, *Energy Environ. Sci.*, 2014, **9**, 2963–2967.
- 9 P. Qin, S. Tanaka, S. Ito, N. Tetreault, K. Manabe, H. Nishino, M. K. Nazeeruddin and M. Grätzel, *Nat. Commun.*, 2014, **5**, 1–6.
- 10 Y. Song, S. Lv, X. Liu, X. Li, S. Wang, H. Wei, D. Li, Y. Xiao and Q. Meng, *Chem. Commun.*, 2014, **96**, 15239–15242.
- 11 X. Liu, F. Zhang, X. Liu, M. Sun, S. Wang, D. Li, Q. Meng and X. Li, *J. Energy Chem.*, 2016, **25**, 702–708.
- 12 J. Guo, X. Meng, J. Niu, Y. Yin, M. Han, X. Ma, G. Song and F. Zhang, *Synth. Met.*, 2016, **220**, 462–468.
- 13 S. Lv, Y. Song, J. Xiao, L. Zhu, J. Shi, H. Wei, Y. Xu, J. Dong, X. Xu and S. Wang, *Electrochim. Acta*, 2015, **182**, 733–741.
- 14 F. Zhang, X. Zhao, C. Yi, D. Bi, X. Bi, P. Wei, X. Liu, S. Wang, X. Li, S. Zakeeruddin and M. Grätzel, *Dyes Pigm.*, 2017, **136**, 273–277.
- 15 F. Zhang, C. Yi, P. Wei, X. Bi, J. Luo, G. Jacopin, S. Wang, X. Li, Y. Xiao, S. M. Zakeeruddin and M. Grätzel, *Adv. Energy Mater.*, 2016, **6**, 1600401.
- 16 F. Zhang, X. Liu, C. Yi, D. Bi, J. Luo, S. Wang, X. Li, Y. Xiao, S. M. Zakeeruddin and M. Grätzel, *ChemSusChem*, 2016, **9**, 2578–2585.
- 17 J. H. Heo, S. H. Im, J. H. Noh, T. N. Mandal, C. S. Lim, J. A. Chang, Y. H. Lee, H. J. Kim, A. Sarkar, M. K. Nazeeruddin, M. Grätzel and S. I. Seok, *Nat. Photonics*, 2013, **6**, 487–492.
- 18 Z. Zhu, Y. Bai, H. K. H. Lee, C. Mu, T. Zhang, L. Zhang, J. Wang, H. Yan, S. K. So and S. Yang, *Adv. Funct. Mater.*, 2014, **46**, 7357–7365.
- 19 Y. Liu, Z. Hong, Q. Chen, H. Chen, W. H. Chang, Y. Yang, T. B. Song and Y. Yang, *Adv. Mater.*, 2016, **28**, 440–446.
- 20 B. Huang, W. Fu, C. Z. Li, Z. Zhang, W. Qiu, M. Shi, P. Heremans, A. Jen and H. Chen, *J. Am. Chem. Soc.*, 2016, **138**, 2528–2531.
- 21 Y. Wang, Z. Yuan, G. Shi, Y. Li, Q. Li, F. Hui, B. Sun, Z. Jiang and L. Liao, *Adv. Funct. Mater.*, 2016, **26**, 1375–1381.
- 22 H. Chen, D. Bryant, J. Troughton, M. Kirkus, M. Neophytou, X. Miao, J. R. Durrant and I. McCulloch, *Chem. Mater.*, 2016, **28**, 2515–2518.
- 23 C. Steck, M. Franckevičius, S. M. Zakeeruddin, A. Mishra, P. Bäuerle and M. Grätzel, *J. Mater. Chem. A*, 2015, **3**, 17738–17746.
- 24 X. Liu, L. Zhu, F. Zhang, J. You, Y. Xiao, D. Li, S. Wang, Q. Meng and X. Li, *Energy Technol.*, 2016, DOI: 10.1002/ente.201600303.
- 25 M. Petrus, T. Bein, T. Dingemans and P. Docampo, *J. Mater. Chem. A*, 2015, **3**, 12159–12162.
- 26 W. Yu, F. Li, H. Wang, E. Alarousu, Y. Chen, B. Lin, L. Wang, M. N. Hedhili, Y. Li, K. Wu, X. Wang, M. F. Mohammed and T. Wu, *Nanoscale*, 2016, **8**, 6173–6179.
- 27 <http://www.sigmaaldrich.com/catalog/product/aldrich/792071?lang=zh®ion=CN>.
- 28 H. Wang, A. D. Sheikh, Q. Feng, F. Li, Y. Chen, W. Yu, E. Alarousu, C. Ma, M. A. Haque, D. Shi, Z. Wang, Q. F. Mohammed, O. M. Bakr and T. Wu, *ACS Photonics*, 2015, **2**, 849–855.
- 29 S. Park, J. H. Heo, C. H. Cheon, H. Kim, S. H. Im and H. J. Son, *J. Mater. Chem. A*, 2015, **3**, 24215–24220.
- 30 A. Krishna, D. Sabba, H. Li, J. Yin, P. P. Boix, C. Soci, S. G. Mhaisalkar and A. C. Grimsdale, *Chem. Sci.*, 2014, **7**, 2702–2709.
- 31 Y. Hua, B. Xu, P. Liu, H. Chen, H. Tian, M. Cheng, L. Kloo and L. Sun, *Chem. Sci.*, 2016, **7**, 2633–2638.
- 32 N. Arora, S. Orlandi, M. I. Dar, S. Aghazada, G. Jacopin, M. Cavazzini, E. Mosconi, P. Gratia, F. De Angelis, G. Pozzi, M. Graetzel and M. K. Nazeeruddin, *ACS Energy Lett.*, 2016, **1**, 107–112.
- 33 M. Cheng, B. Xu, C. Chen, X. Yang, F. Zhang, Q. Tan, Y. Hua, L. Kloo and L. Sun, *Adv. Energy Mater.*, 2015, **8**, 1808–1810.
- 34 X. Zhao, S. Wang, Y. You, Y. Zhang and X. Li, *J. Mater. Chem. C*, 2015, **34**, 11377–11384.
- 35 S. Lv, Y. Song, J. Xiao, L. Zhu, J. Shi, H. Wei, Y. Xu, J. Dong, X. Xu, S. Wang, Y. Xiao, Y. Luo, D. Li, X. Li and Q. Meng, *Electrochim. Acta*, 2015, **182**, 733–741.
- 36 A. Krishna, D. Sabba, H. Li, J. Yin, P. Boix, C. Soci, S. G. Mhaisalkar and A. C. Grimsdale, *Chem. Sci.*, 2014, **5**, 2702–2709.
- 37 Y. Shi, K. Hou, Y. Wang, K. Wang, H. Ren, M. Pang, F. Chen and S. Zhang, *J. Mater. Chem. A*, 2016, **4**, 5415–5422.
- 38 W. H. Nguyen, C. D. Bailie, E. L. Unger and M. D. McGehee, *J. Am. Chem. Soc.*, 2014, **31**, 10996–11001.
- 39 G. D. Niu, X. D. Guo and L. D. Wang, *J. Mater. Chem. A*, 2015, **17**, 8970–8980.